Supporting 5G Wireless Networks Through IEEE802.11ac Standard With New Massive MIMO Antenna System Module Design in Omnet++ Simulator

Vincenzo Inzillo[1], Floriano De Rango[1] and Alfonso Ariza Quintana[2]
[1]*DIMES, University of Calabria, via P. Bucci, Rende (CS), Italy*
[2]*University of Malaga, av. De Cervantes, Malaga, Spain*

Keywords: 5G, Massive MIMO, Ieee802.11ac, Beamforming, Antenna, Omnet++.

Abstract: The advances accomplished in the modern wireless network design are requiring increasingly more efficient high-performing antenna devices in order to satisfy the requirements provided for the 5G next generation systems; although a considerable number of theoretical proposals already exist in this field the most common used network simulators do not offer a support for the latest wireless network standards such as the IEEE802.11ac and, at the same time, they do not afford the possibility to utilise the latest up-to-date high performance massive MIMO (Multiple Inputs Multiple Output) antenna systems. In view of this, we propose to extend the basic feature offered by the Omnet++ network simulator with the aim of actualizing the current simulation instruments for enabling the emulation of 5G wireless network scenarios.

1 INTRODUCTION

In the latest years, the need for satisfying high requirements relating to the management of wireless traffic is constantly rising. Basically, the most common and simple technology for wireless communication systems deals with the use of a single antenna either in transmission and in reception. These kinds of systems are usually known as SISO (Single Input Single Output). However, nowdays, significant advances have been accomplished in this field in order to create more complex and efficent systems which are able to improve the performance of the traditional tecnhology; the result has been the evolution of more articulated mechanisms such as the MIMO technology which provide for the use of multiple antennas for both the transmitter and the receiver with the aim to considerably improve the SISO performance (Björnson et al., 2015), (Larsson et al., 2014), (El Ayach et al., 2014). In literature, many researches have been demonstrated how the use of directional antennas and the most recent SAS (Smart Antenna Systems) technology is capable of significantly allow high QoS (Quality of Service) requirements in spite of the omnidirectional systems that foresee limited functionalities (Jain and Agarwal, 2016), (Senapati et al., 2015), (Kumar et al., 2014). The benefits of directional antennas can be exploited also in vehicular environments (Fazio et al., 2012),(Fazio et al., 2011). Therefore, using high efficency antenna systems combined with scalable routing protocol could favourite the improvement of the overall network performance (Zhou et al., 2006), (De Rango et al., 2006), (De Rango et al., 2008), and can positively impact on the energy consumption encouraging e better exploitation of the power resources with respect to the omnidirectional case (Nguyen et al., 2016a), (Nguyen et al., 2016b). However, these solutions are unlikely to fulfil the requirements for the the 5G next generation wireless communication systems technology. For this purpose, the massive MIMO technology has been proposed as efficient solution for satisfying the requirements for 5G that certainly include very high antenna gain and very high data rate in order to achieve huge system performance (Lu et al., 2014), (Gao et al., 2015), (Molisch et al., 2017). The term massive, means that this kind of systems use a large number of antenna

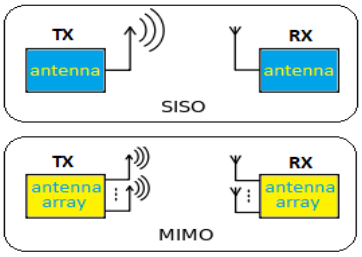

Figure 1: SISO and MIMO example schema.

Inzillo, V., Rango, F. and Quintana, A.
Supporting 5G Wireless Networks Through IEEE802.11ac Standard With New Massive MIMO Antenna System Module Design in Omnet++ Simulator.
DOI: 10.5220/0006910800620072
In *Proceedings of 8th International Conference on Simulation and Modeling Methodologies, Technologies and Applications (SIMULTECH 2018)*, pages 62-72
ISBN: 978-989-758-323-0

elements in the hardware architecture; indeed, relating to the modern wireless networks, for achieving high communication benefits in terms of throughput we need for a massive number of elements that is not less than 70-80 antennas (Björnson et al., 2016). The main reason for that is because, theoretically, as the number of elements improves also the overall gain of the system increases, in fact, each single antenna element contributes to enhance the total gain. More specifically, from the antenna array theory is well known that the overall gain is affected by the single element factor as well as the array factor and this gain increases with the number of antenna elements. The massive MIMO are strongly recommended for beamforming environments by the most recent IEEE802.11n and IEEE802.11ac standards. One of the most known issue related to 5G wireless communication systems is represented by the fact that, actually, only a very limited number of network simulators allow to emulate these very complex technologies; in the same way, there exist very few network simulators that enable the requirements provided by the recent IEEE802.11 standards such as the IEEE802.11ac. Unfortunately, in such cases, with regard to these network simulators, the cost of the license allowing the end user to access to the 5G package modules, could result very expensive (Mezzavilla et al., 2015), (Zhang et al., 2017). For this reason, in the present paper, we propose to enhance the features of one of the most open source network simulator, that is the *Omnet++* network simulator (Omnet++, 2018), in order to provide a support either for a massive MIMO antenna system and either for emulating a network environment in line with the latest release of the IEEE802.11ac standard.

2 THE MASSIVE MIMO SYSTEMS

Massive MIMO is a rising technology, that considerably enhances the basic MIMO features. With massive MIMO, are usually indicated the whole of systems that uses antenna arrays with at least few hundred antennas, simultaneously serving multiple terminals in the same time frequency resource.
The Fig. 2 illustrates the basic operating principle of a massive MIMO; few users are served from a macro-device having a large number of base stations (antennas). Generally, massive MIMO is an instrument that allows to enable the development of future broadband (fixed and mobile) networks which will satisfy special requirements in terms of energy efficiency, security, and robustness. At the same way, they will represent a lever for the future digital society infrastructure that

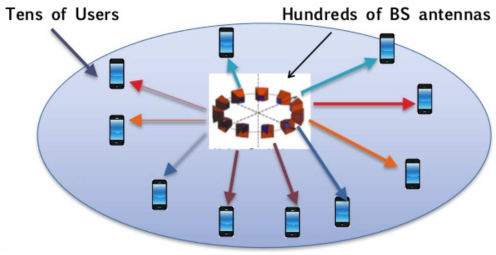

Figure 2: Massive MIMO operation principle.

will connect the Internet of people, Internet of Things, clouds and other network infrastructure. In terms of architecture, a massive MIMO system consists of a group of small (relatively) antennas, supplied from an optical or electric digital bus that operates simultaneously related to a certain task. Massive MIMO, as well as the SAS systems are able to well exploit the SDMA (Spatial Division Multiple Access) allowing for an efficient resource channel utilization, both on the uplink and the downlink (Yan and Cabric, 2017), (Yang et al., 2015). In conventional MIMO systems, like the LTE (Long Term Evolution), the base station transmits waveforms depending on terminals channel response estimation, then, these responses are quantized by some processing units and sent out back to the base station. Fundamentally, this is not possible in massive MIMO systems (Zhang et al., 2015), especially concerning high-mobility environments (Jungnickel et al., 2014), because optimal downlink pilots should be mutually orthogonal between the antennas. In other words the amount of time frequency resources needed for downlink scales as the number of antennas, so a massive MIMO system would require a burden of resources up to a hundred times more than a conventional system. Therefore in spite of the difficult hardware and designing implementation, these systems are becoming increasingly prevalent in the modern applications due to the great benefits that could introduce:

- Massive MIMO can increase the wireless channel capacity up to 10 times with respect to the traditional LTE systems. This means very high coverage.
- Massive MIMO can improve the radiated energy-efficiency up to 100 times with respect to the traditional LTE systems. This translates into higher gains and higher performance.
- With large number of antennas, the energy can be focused with extreme sharpness into small regions in space. This feature encourages a better energy system resource exploitation.
- Limited designing costs, if low power components are used.

However, the employement of these systems entails a series of issues that should be properly considered:

- Interferences between terminals increase as the data rate increases. However, techniques as the ZF (Zero Forcing) could be used to suppress such interferences.
- The terminals consume a lot of energy during the communication process in spite of the well SDMA exploitation.
- The difficult for designing a system of limited size grows up with the number of antennas. For this reason it is necessary to find a trade-off between the number of elements and the requirements.

3 MASSIVE MIMO

From an architectural point of view, a massive MIMO is structured depending on the geometry pattern that is able to form. There exist several design configurations that usually are function of the kind of application to which these systems are destined. Anyway, in this paper, we consider three different types of planar antenna arrays: the URPA, the UHPA and the UCPA. The following subsection synthetizes the main feature of the mentioned configurations.

3.1 Massive MIMO URPA

The Uniform Rectangular Planar Array technology, is the most simple planar massive MIMO configuration. The geometry pattern in this case is consist of a simple matrix within which the antenna elements are placed. The Fig. 3 illustrates an example of massive

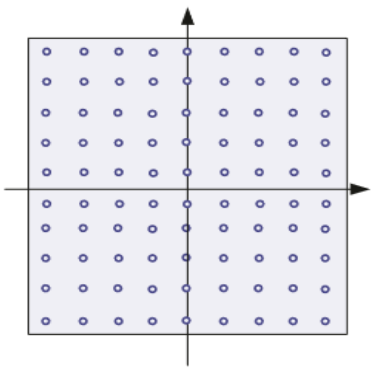

Figure 3: Massive MIMO URPA example.

MIMO URPA configuration. Basically, a URPA is a two-dimensional matrix filled with a certain number of antenna elements (the circles in the figure) both along the x and the y axis; these antenna elements are equally spaced between each one and this spacing is usually expressed in wavelengths. If we denote the number of elements placed on the x axis with M (the rows of the matrix) and with N the number of antennas lying in the y axis (the columns of the matrix), the total number of elements of the URPA is given from:

$$NumElements = M \times N \tag{1}$$

Where M and N are arbitrary integers typically higher than 1. In the first versions of the URPA, M and N were identical and limited to 8; in the modern application M and N are commonly different and chosen between 8 and 12. In general, the radiation field formed by the antenna elements (known also with the term *element factor*) is given by:

$$E_m(r,\theta,\phi) = Af(\theta,\phi)\frac{e^{-jkr}}{r} \tag{2}$$

Where A is the nominal field amplitude, $f(\theta,\phi)$ is the radiation field pattern , and r is the radial distance between the element and the reference point, that highlights the decrease of the field in function of the distance. According to the pattern multiplication principle, the antenna array total electrical field can be expressed as:

$$E_{TOT} = E_m \times AF(\theta,\phi) \tag{3}$$

In eq. 3, the term $AF(\theta,\phi)$ is also known as *array factor* and it depends on the geometry structure of the array. In the case of URPA, the array factor equation is very similar to the Uniform Linear Array (ULA) with the only difference that is designed by considering two dimensions:

$$AF_{URPA}(\theta,\phi) = \left[\frac{\sin\left(\frac{M\psi_M}{2}\right)}{\sin\left(\frac{\psi_M}{2}\right)}\right]\left[\frac{\sin\left(\frac{N\psi_N}{2}\right)}{\sin\left(\frac{\psi_N}{2}\right)}\right] \tag{4}$$

With:

$$\begin{aligned}\psi_M &= kd\sin\theta\cos\phi + \beta_M \\ \psi_N &= kd\sin\theta\sin\phi + \beta_N\end{aligned} \tag{5}$$

Where:

$$\begin{aligned}\beta_M &= -kd\sin\theta_0\cos\phi_0 \\ \beta_N &= -kd\sin\theta_0\sin\phi_0\end{aligned} \tag{6}$$

In the eq. 5 the terms ψ_M and ψ_N indicate the array phase along the x and the y axis respectively while the terms β_M and β_N denote the scanning steering factors along x and y in function of the steering angle θ_0; finally, ϕ_0 is the azimuthal elevation steering angle term. Observe that the array factor expression related to eq. 4 is not normalized with respect to M and

N. The overall gain of the URPA is expressed by the following:

$$G(\theta,\phi) = \frac{4\pi|f(\theta,\phi)AF(\theta,\phi))|^2}{\int_{\phi=0}^{2\pi}\int_{\theta=0}^{\pi}|f(\theta,\phi)AF(\theta,\phi))|^2\sin\theta\, d\theta d\phi} \quad (7)$$

The eq. 7 is the generic expression of the gain valid for all antenna types and is function of the element factor and the array factor. If the antenna elements are isotropic we have $f(\theta,\phi) = 1$ and the gain becomes :

$$G(\theta,\phi) = D(\theta,\phi) = \frac{4\pi|AF(\theta,\phi))|^2}{\int_{\phi=0}^{2\pi}\int_{\theta=0}^{\pi}|AF(\theta,\phi))|^2\sin\theta\, d\theta d\phi} \quad (8)$$

The eq. 8 also expresses the directivity of the antenna; thus, from antenna array theory it is possible to obtain the expression which correspond the maximum gain in case of isotropic antenna elements:

$$G_{MAX}(\theta,\phi) = \frac{4\pi\times NumElements^2}{\int_{\phi=0}^{2\pi}\int_{\theta=0}^{\pi}|AF(\theta,\phi))|^2\sin\theta\, d\theta d\phi} \quad (9)$$

Indeed, the maximum gain is the value corresponding to the maximum value of the array factor that in the case of the URPA is:

$$AF_{MAX}(URPA) = AF_{MAX}(ULA) = NumElements \quad (10)$$

Note that the maximum value of the array factor for URPA is the same for the ULA and it is equal to the total number of elements of the system. However, from theory, it is known that in the eq.9 it is not possible to approximate the term $AF(\theta,\phi))$ to *NumElements* because is function of θ and ϕ which in turn determine the dependency parameters of the double integral.

4 THE IEEE802.11ac STANDARD OVERVIEW

In the latest years, the improvements related to the gigabit wireless communications contribute to develop the IEEE802.11 WLAN standards. In 2010,the Wireless Gigabit (WiGig) Alliance, defined a unified architecture for enabling tri-band communications over the frequency bands of 2.4, 5, and 60 GHz. The most recent standards such as 802.11n and 802.11ac are developed according the WiGig specifications and enhance the features offered 802.11b/a/g standards that are designed for bands of 2.4 and 5 GHz. Actually, the latest release of the IEEE802.11ac could provide a maximum physical data rate of about 7 Gbps. In other terms, the standard deals with a throughput higher than 500 Mbps for a single user scenario and an aggregated MAC throughput of more than 1 Gbps for a multi-user scenario, both using less than 80 MHz of channel bandwidth. Consequently, 802.11ac is destined for higher data rate applications such as Ultra High Definition (UHD) television, wireless implementation of high-definition multimedia interface (HDMI replacement), and lately, the wireless display applications. Globally, 802.11ac could be considered as an extension of 802.11n in which the two basic notions of MIMO and wider channel bandwidth are improved. Compared to 802.11n, the IEEE80211.ac increases the theoretical maximum physical data rate by a twice factor proportional to the number of spatial streams or channel bandwidth. Therefore, 802.11ac defines the specifications for supporting VHT (Very High Throughput) features in terms of devices, beamforming, spectral mask, data rate, modulations and coding. The main specifications provided by the IEEE802.11ac for the VHT are listed as follows:

- Frequency range: 5 GHz.
- Modulation Scheme: OFDM and DSSS/CCK.
- Supported data modulations: BPSK, QPSK, 16-QAM, 64-QAM, 256-QAM.
- Channel Bandwidth: 20 MHz, 40 MHz, 80 MHz, 160 MHz.
- Supported coding rate: coding rate of 1/2, 2/3, 3/4, and 5/6.
- Short guard interval: 400 ns, 800 ns.
- Maximum supported number of spatial streams: 8.
- Maximum supported data rate: 6.93 Gbps using 160 MHz bandwidth.

The IEEE802.11ac has increased the number of Spatial Streams from 4 (802.11n) up to 8 relating to the use of the OFDM (Orthogonal Frequency Division Multiplexing). There are several advantages of using more MIMO in 802.11ac, such as very extended communication range, high reliability, very high throughput. The standard also supports downlink MU (Multi User) MIMO which provides that an AP (Access Point) can send multiple data frames in the form of Aggregated MAC Protocol Data Unit (A-MPDU) to multiple receivers at the same time. A more advanced modulation such as the 256-QAM (Quadrature Amplitude Modulation) has been added to 802.11ac standard. This increases the number of bits per subcarrier of OFDM compared to 64-QAM. As a result, the data rate raises up to 33% as compared to previous 802.11 standards. On one hand it significantly increases data rate; on the other hand, however, it requires higher Signal to Noise Ratio (SNR) for recei-

vers to correctly demodulate the symbols. Similarly, 802.11ac supports various coding rates. With 5 GHz band, the bandwidth of 802.11ac has been increased. In addition to 20 MHz and 40 MHz channels that were already available in 802.11n, wider channels of 80 MHz and 160 MHz have been added in 802.11ac. Furthermore the 160 MHz channel can be established with two contiguous or non-contiguous 80 MHz channels. The Table 1 depicts the allowed 802.11ac con-

Table 1: VHT confs. for 160 MHz and 80+80 MHz, N_{SS}=8.

ind.	Mod.	CR	Data rate (Mbps)	
			800 ns GI	400 ns GI
0	BPSK	1/2	468	520
1	QPSK	1/2	936	1040
2	QPSK	3/4	1404	1560
3	16-QAM	1/2	1872	2080
4	16-QAM	3/4	2808	3120
5	64-QAM	2/3	3744	4160
6	64-QAM	3/4	4212	4680
7	64-QAM	5/6	4680	5200
8	256-QAM	3/4	5616	6240
9	256-QAM	5/6	6240	6933.3

figurations for VHT related to the maximum physical parameter values settings that provides for 8 Spatial Streams (N_{SS} = 8) at the optional 160 MHz band or by using two 80 MHz channels. From the table it can be highlighted that in the best permitted configuration, by using a 256-QAM with coding rate of 5/6 and a GI (Guard Interval) of 400 ns, it is possible to achieve a data rate of about 7 Gbps. Anyway, in the latest 802.11ac draft, the specifications suggest that it is possible to achieve data rates higher than 10 Gbps if 512-QAM and 1024-QAM are used (according to the 5G network operation requirements). The IEEE802.11ac standard also defines the specifications about the devices to be employed in order to achieve the data rates of Tab. 1; more specifically, the beamforming section of the standard, indicates the use of MU-Massive MIMO systems containing a number of antenna elements proportional to the number of Spatial Streams.

5 PROPOSED MODEL AND MOTIVATIONS

The latest release of the *Omnet++* simulator (the 5.3 version), does not provide neither for a support to asymmetrical communications and neither for the implementation of the latest IEEE802.11 standards. However, as regards the first aspect, we already designed in (Inzillo et al., 2017b) a *PhasedArray* SAS module that allows to emulate asymmetrical directional communications also enabling simulation beamforming scenarios. As regards the second aspect, indeed, *Omnet++* offers a complete support for 802.11b/g and the most recent 802.11n standard; in particular, the latest version of *Omnet++* implements various beamforming features of the 802.11n such as the MAC frame aggregation. Nevertheless, these features are not sufficient for emulating the latest massive MIMO technologies that require the complete design of the IEEE802.11ac standard in terms of physical layer features. In fact, the maximum data rate supported in the radio module by the current latest version of *Omnet++* is 54 Mbps, along with a 64-QAM modulation, according to the 802.11n specifications. In view of these issue we aim to extend the *Omnet++* features both by providing a full 802.11ac radio environment and a new massive MIMO antenna module suitable for 5G wireless network environments operating according to the IEEE802.11ac standard.

5.1 IEEE802.11ac Implementation

The first step consists in the implementation of the 802.11ac standard in the physical modules of *Omnet++*. Basically, this process involves modifications as regards two micro-layers: the *error model* and the *modulation*. The error model determines the computation of the BER (Bit Error Rate) and PER (Packet Error Rate) curves and furthermore the error probability evaluation in function of the data rate configurations. Obviously, as already stated, the current error models are determined by considering the maximum data rate of 54 Mbps. For this reason, this aspect should be fixed in order to design a support of data rates in the order of the Gbps. The modulation is the feature that offers the possibility to achieve the data rate values specified for VHT and in the current latest version *Omnet++* is limited to 64-QAM; this aspect determines the data rate upper-bound in the simulations. The family of modules related to the error model and modulation are contained in the *physicallayer* package of the *Inet* framework provided by *Omnet++*.

The Fig. 4 illustrates the structure of the *physicallayer* package. The package consists of a remarkable number of subpackages each one determining a feature for the physical layer. Observe that the error model and the modulation micro-layers are contained in this package along with main modelling channel attributes, such as the propagation and the pathloss management. Thus, in order to understand updates introduced for implementing the IEEE802.11ac standard, the following figures show a block diagram including

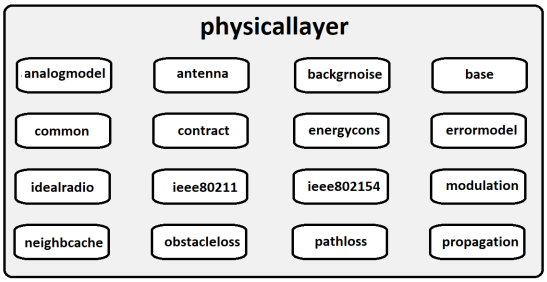

Figure 4: Physicallayer Omnet++ package structure.

the main *Omnet++* classes (known also as *modules*) involved in the modification process.

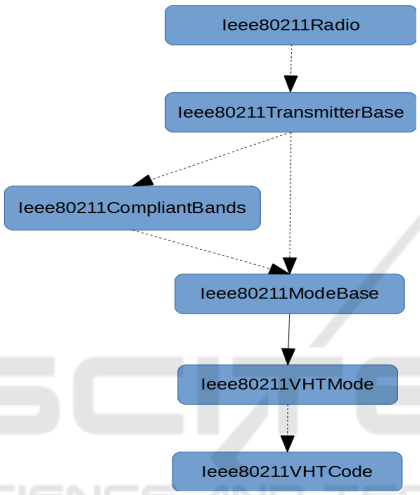

Figure 5: VHT implementation in the transmitter.

The Fig. 5 represents the module block diagram related to the implementation of the VHT features for the transmitter at physical layer. Each class/module is represented by a rectangle while the dashed-line arrows and the continued-line arrows indicate the *use* and the *inheritance* relationship respectively. The *Ieee80211Radio* module uses the *Ieee80211TransmitterBase* module that is defined by the following NED (Network Description Language) code lines:

Listing 1: Ieee80211TransmitterBase.ned definition.

```
1 module Ieee80211TransmitterBase ... {
2 string opMode @enum("a", "b", "g(erp)", "g(mixed)", "n(
      mixed-2.4Ghz)", "p", "ac");
3 string bandName @enum("2.4 GHz", "5 GHz","5 GHz&20 MHz"
      ,"5 GHz&40 MHz","5 GHz&80 MHz","5 GHz&160 MHz");
4 int channelNumber;
5 modulation = default("BPSK"); }
```

In the Listing 1 the main parameters of the *Ieee80211TransmitterBase* module are illustrated. The *opMode* parameter indicates the kind of IEEE802.11 standard that is determined by a lowercase letter. In this regard, we modified the default code by adding the ac operation mode. Note that also the 5 GHz frequency band configurations have been added. The transmitter uses the class *Ieee80211CompliantBands* for retrieving the available bands and the *Ieee802ModeBase* class obtaining the operation mode. This latest class inherits the parameters offered by the classes *Ieee80211VHTMode* and *Ieee80211VHTCode* that contains the new data rate values specified by the 802.11ac standard according to the VHT specifications. For this purpose we added all the data rate values provided by the standard by varying the carrier frequency and the number of spatial streams (a small part of these values are illustrated in the Table 1). The *Ieee80211VHTCode* is the module that computes the error probability functions depending on the kind of modulation used in simulation. A similar block diagram could be designed for the receiver.

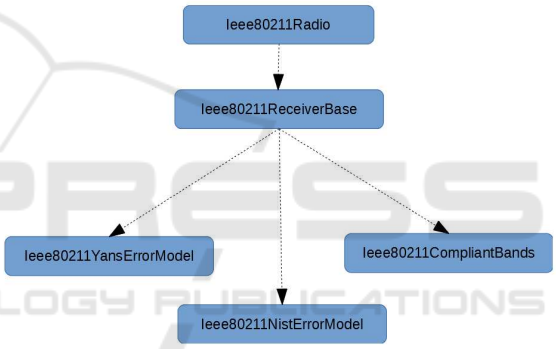

Figure 6: Error model designing at the receiver.

In the diagram of Fig. 6 it is possible to analyze the hierarchical relationships at the receiver. It is important to highlight that the error model is mainly used by the receiver rather than the transmitter. *Omnet++* uses some of the error models offered from the *NS3* simulator (Carneiro, 2010) that are the Yans and the Nist models (Pei and Henderson, 2010). Basically, these error modules compute the BER probability values in function of the modulation. For enabling the 802.11ac we extended the default code of *Omnet++* by adding the BER computation functions for 256, 512 and 1024-QAM modulation:

Listing 2: Nist error model BER computation example.

```
1 double Ieee80211NistErrorModel::get256QamBer (double
      snr) const {
2  double z = std::sqrt (snr / (85.0 * 2.0));
3  double ber = 15.0 / 32.0 * 0.5 * erfc (z);
4  EV << "256-Qam" << " snr=" << snr << " ber=" << ber;
5  return ber; }
```

The Listing 2 contains a piece of the full code of the *Ieee80211NistErrorModel* class. The function *get256QamBer* computes and returns the BER relating to a 256-QAM modulation; the BER is evaluated by computing the Zeta function that depends on the SNR (Signal to Noise Ratio).

5.2 Massive MIMO URPA Design and Implementation

Once that we modified the physical layer in order to support the specifications of the VHT standard including the error model and modulations, we designed the massive MIMO antenna module. The antenna modules are defined in the *phyisicallayer* package as depicted in Fig. 4. Actually the available antennas in the physicallayer package are:

- **ConstantGainAntenna**: a simple antenna having a unique basic parameter: the gain. As suggested by the name the gain set in the configuration file remains constant while a simulation run is executed.
- **CosineAntenna**: it is the cosine pattern antenna designed in (Chunjian, 2003); this model results very usefully for W-CDMA systems.
- **DipoleAntenna**: the well-known dipole antenna. It consists of two identical conductive elements, which are bilaterally symmetrical; it is possible to set in the configuration file the length of the dipole (expressed in meters).
- **InterpolatingAntenna**: this antenna model computes the gain in function of the direction of the signal, using linear interpolation.
- **IsotropicAntenna**:it is the classical omnidirectional/isotropic antenna; it provides for unity gain by radiating the signal at the same way towards all directions.
- **ParabolicAntenna**: this model is based on a parabolic approximation of the main lobe radiation pattern. The gain is function of the *maxGain* and the *minGain* together with the 3db beamwidth.
- **PhasedArray**: the SAS model that we designed in (Inzillo et al., 2017b). We provided either for a switched beam version and either for a adaptive array configuration (Inzillo et al., 2017a).
- **MassiveMIMOURPA**: the massive MIMO URPA module which represents one of the task performed in the present paper and that will be explained in the current section.

The latest two antenna modules enhance the default features of *Omnet++* because they provide for a support for asymmetrical and directional communications scenarios. Anyway, the detailed description of all kinds of antennas is beyond the scope of this paper which instead aims to illustrate the designing feature of the *MassiveMIMOURPA* module.

Listing 3: MassiveMIMOURPA.ned definition.

```
module MassiveMIMOURPA extends AntennaBase {
   parameters:
       double length @unit(m); // length of the antenna
       double distance; // distance between elements
       double freq; // frequency
       double phiz; // steering angle
       int M; //number of columns
       int N; //number of rows
       .......}
```

The listing 3 illustrates the main definition parameters of the *MassiveMIMOURPA* antenna module. Note that the module inherits the basic features of the *AntennaBase* module; besides the main antenna array parameters such as the *length* the *distance* and the *frequency* the module provides for the setting of the steering angle *phiz* in order to support the beam piloting; as already mentioned in the subsection 2.1, M and N represent the number of elements to be placed on the y-axis and x-axis respectively. Therefore, the logic operations of the module are defined in the *.cc* file which can be synthesized by the following pseudo-code:

Algorithm 1: MassiveMIMOURPA.cc pseudo-code.

procedure INITIALIZE(int *stage*)
    initialize the module
end procedure

procedure GETMAXGAIN
    double *maxG*;
    int *numel* = *getNumAntennas*();
    double *numer* = $4 * M_{PI} * numel * numel$;
    $maxG = 20 * log10(numer/risInt)$;
    return *maxG*;
end procedure

procedure COMPUTEGAIN(EulerAngles *direction*)
    double $k = (2 * M_{PI})/lambda$;
    double $phizero = phiz * (M_{PI}/180)$;
    double $heading = direction.alpha$;
    double $elevation = direction.beta$;
    double $psiM = (k * d * sin(heading) * cos(heading)) + (-k * d * sin(phizero) * cos(phizero))$;
    .....
    return *gain*;
end procedure

procedure COMPUTEINTEGRAL
    double *risInt* = computes the double integral
    return *risInt*;
end procedure

The Algorithm 1 defines the main functions of the *MassiveMIMOURPA.cc* class. The function *getMax-*

Gain compute the maximum gain according the to the eq. 9; the function *getNumAntennas* returns the total number of antennas of the massive MIMO; the result of double integral (given by the *risInt* variable) is evaluated by implementing the Simpson method (Ohta and Ishida, 1988) in C++ in the function *computeIntegral*; Observe that the integral could be computed by using some mathematical software tools as MATLAB and then passed to *Omnet++*, but in this case, we decided to implement the evaluation in C++ because the computation is once and because the use of MATLAB with this kind of very complex antenna module could significantly slow down the simulation. Finally, the function *computeGain* evaluates the gain in function of the direction *EulerAngles* components (Janota et al., 2015) and the steering angle *phiz* according to the eq. 8; indeed we assumed that the single antenna elements are isotropic. The *computeGain* function evaluates the gain through the definition of some parameters such as the wavenumber *k* that is function of the wavelength *lambda*; however, the components along the θ and ϕ cuts are extracted by considering the *alpha* and *beta* components related to the *direction* that is the input argument of the function.

6 MODEL VALIDATION AND SIMULATION RESULTS

The validation of the designed models is accomplished by illustrating some log screens related to the debug runs and by analyzing some useful statistics extracted from the simulations. The following table includes the most important simulation set parameters:

Table 2: Main simulation parameter set.

Antenna Model	Massive MIMO URPA
Network Standard	Ieee802.11ac
Num. of elements	90 (M = 9, N = 10)
Steering angle	45°
Elem. Spacing	0.5 λ
Carrier freq.	5 GHz
Ch. bandwidths [Mhz]	20, 40, 80, 160
Data Rates [Mbps]	from 57.8 to 6933.3
Traffic data type	UDP
Message Length	512 *Byte*
Network Load	50 %
Sim. Area Size	500 x 500 *m*
Sim. time	300 *s*
Num. of repetitions	20

The simulations have been accomplished by using 20 different seeds and extracting the confidence intervals obtained by the repetitions considering a confidence level set to 95 %. The traffic is represented by UDP (User Datagram Protocol) data packets randomly generated (based on the simulation seed) by different couples of nodes. The number of spatial streams (N_{SS}) is set to 8. Therefore, the most of the antenna parameters including the number of elements and the spacing in the system are the same used in (Tan et al., 2017) with the only exception that we also provided for the beam steering angle setting. For simulations we considered such of the data rates provided by the 802.11ac standard in function of the number of spatial streams. In order to validate the model, the first test consists of the analysis of such run simulation logs:

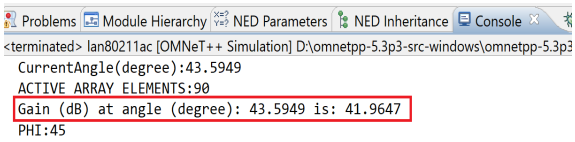

Figure 7: Portion of log extracted by simulations.

Fig. 7 represents a portion of log extracted by a randomly chosen simulation run; the result of the log is printed on the console perspective of Omnet++; the red rectangle highlights the main line of the log, that displays the result of the computed gain in function of the current angle; the main line synthesizes that the value of the gain corresponding to the angle of 43.5949 ° is 41.9647 dB; considering the steering angle of 45° we can manually compute the maximum gain that is the gain corresponding to the maximum radiation angle (thus the steering angle) by using the eq. 9 and replancing the terms of the equation with the values used in Tab. 2:

$$G_{MAX} = \frac{4\pi \times 90^2}{772.97} - \delta_{steer} = \mathbf{42.16\ \ dB} \qquad (11)$$

Where δ_{steer} represents the attenuation in dB related to the steering angle with respect to the maximum gain corresponding to $\theta = 0°$ (which is 42.39 dB). In the eq. 11, the value of 772.97 at the denominator is the result of the double integral computed by the simulator, using the Simpson method. The same result could be easily computed by using the following MATLAB code:

Listing 4: Double integral MATLAB code.

```
1 fun = @(x,y)((((sin(0.5.*9.*pi.*sin(x).*cos(y))))./(sin
      (0.5.*pi.*sin(x).*cos(y)))).*((sin(0.5*10.*pi.*sin
      (x).*sin(y))))./(sin(0.5.*pi.*sin(x).*sin(y)))))
      .^2).*sin(x);
2 q = integral2(fun,0,pi,0,2*pi);
```

Finally, the gain value of 41.9647 dB obtained in the log related to the angle of 43.5949 ° (that is an angle

very near to the steering angle) is almost about close to the maximum gain value, as we could expect. For a further investigation it is possible to design the same considered massive URPA by using the Sensor Array Analyzer tool provided by MATLAB and compare the values obtained in our case.

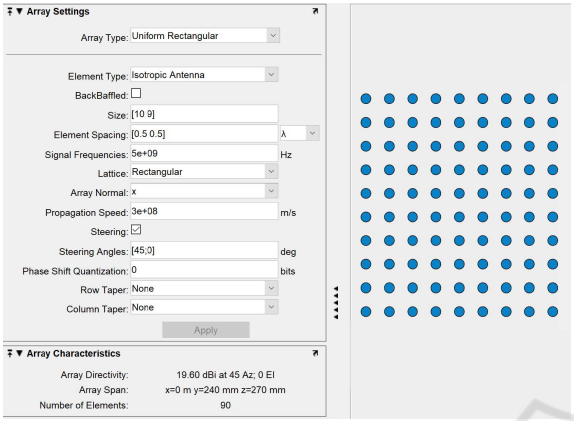

Figure 8: Designed model using Sensor Array Analyzer.

The Fig. 8 displays the configuration related to our designed antenna model generated by the Sensor Array Analyzer. In the figure, the value of the maximum gain is the value related to the directivity that is 19.60 dBi (power dB value) which corresponds approximately to 42.16 dB. This value is exactly the same value obtained in our simulations. The second phase of the model validation involves the analysis of such simulation statistics extracted from runs. For this purpose we performed the runs by increasing the data rate as well as the channel bandwidth. More specifically, we considered the following configurations:

- **for 20 MHz** : 57.8 and 115.6 Mbps
- **for 40 MHz** : 360 and 720 Mbps
- **for 80 MHz** : 1560 and 2340 Mbps
- **for 160 MHz** : 5200 and 6933.3 Mbps

Note that the data rate is increased about twice between each configuration. The used data rate values are extracted from the IEEE802.11ac standard related to the tables having $N_{SS} = 8$ and guard interval of 400 ns. The first analyzed statistic is related to the average SNIR (Signal to Noise Interference Ratio) in function of the data rate and is derived by extracting the *minSNIR* statistic provided by *Omnet++*. The values extracted from the minSNIR histogram are averaged by considering 3 different values of power for the transmitter : 40, 70 and 100 mW. Also consider that we performed the simulations by using a value of background noise set to -110 dbm. This value suggests that the channel is weekly affected from interferences.

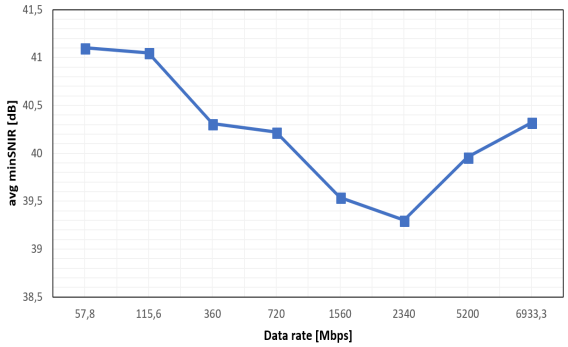

Figure 9: Average minimum SNIR vs data rate.

The Fig. 9 illustrates the average minimum SNIR in function of the data rate. The best case, as we can expect, is registered at the low data rate case; as the data rate enhances the SNIR tends to decrease almost linearly according to the theoretical expectations. However, observe that corresponding to the highest data rates the decreasing trend seems to reverse. This is probably due because of two main reasons: firstly, the bandwidth amplitude related to these two data rates which is at least double with respect to the other configurations; secondarily, the level of the modulations used for the data rates 5200 and 6933.3 that are a 64-QAM and a 256-QAM respectively, which can grant similar performance compared to lower data rates configurations that use less efficient modulation schemas, especially when the channel is very weekly affected from noise. The second statistic also concerns the SNIR but in this case is evaluated in function of the power at the transmitter:

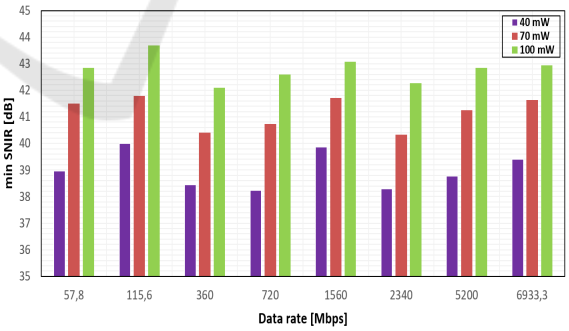

Figure 10: Minimum SNIR vs power and data rate.

In the Fig. 10 the *minSNIR* is evaluated in function of the power at the transmitter by increasing the data rate. Observe that in this case, the values are scalars and are averaged only in function of the simulation repetitions. As we can expect, the higher is the power, the more is the SNIR in all data rate cases; the difference between each power transmission case is holding steady. The latest statistic that we studied is related to the throughput of the designed massive

MIMO antenna model; the throughput curve in this case is averaged with respect to the data rates. In this field we performed other 3 different simulation runs that differ from the previous as regards the kind of used antenna in the nodes (the data traffic instead, remains the same). In particular, we replaced the *MassiveMIMOURPA* with the *PhasedArray* ULA module that we designed in (Inzillo et al., 2017b); then we compared the massive MIMO curve with 3 different *PhasedArray* cases: 10, 15 and 20 elements in the array. The values are obtained by averaging the vector throughput statistics provided by *Omnet++* generated by the *thruputmeter* module.

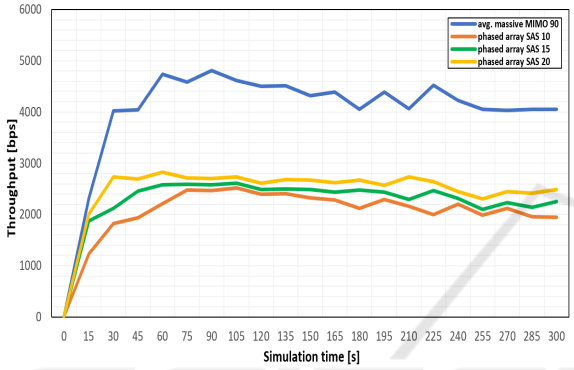

Figure 11: MassiveMIMOURPA and PhasedArray throughput comparison.

In the Fig. 11 we compared the throughput curves by using the two considered antennas. Observe how, when the *MassiveMIMOURPA* module is used , the average throughput is about double with respect to the best *PhasedArray* case. Obviously the reasons of this result are clear and include: the gain, the number of elements, the bandwidth and the carrier frequency. Finally, it can be noted that, as the number of the *PhasedArray* antenna elements grows up, the throughput slightly increases according to the expectations; anyway, in the best *PhasedArray* case (20 antenna elements) we registered an average throughput of 2.3 Mbps against the 4.7 Mbps value obtained in the *MassiveMIMOURPA* case.

7 CONCLUSIONS

We proposed a simulation model that allows to extend the default features of the *Omnet++* network simulator in order to implement the IEEE802.11ac standard. This last one is useful for the analysis at physical layer of the network devices provided by the 5G next generation wireless network systems. For this purpose, we modified some module of the *physical-layer* package extending the default Nist error model and inserting all the features provided by the 802.11ac standard in terms of modulations and data rates. Furthermore, for validating the model, we designed a new *MassiveMIMOURPA* module for verifying the operation of the implemented standard. The simulation logs and the simulation results have shown that, the designed model works according the theoretical expectations. In particular, the model has been compared with the Sensor Array Analyzer tool provided by MATLAB that confirmed the correctness of the model in terms of gain computation; Secondarily, we analyzed the statistics generated by *Omnet++* also making some comparisons in terms of throughput when a different antenna module is used. For this purpose we replaced the massive MIMO designed module with the *PhasedArray* SAS module. The main goal of the present paper was to provide for an open source simulation instrument for the emulation of the future wireless network scenarios, in order to overcome the main issues in this field, including the expensive license costs of the very few simulation companies that offer these kinds of features; at the same way, this work aims to upgrade the set of features offered by *Omnet++* for the purpose of enhancing the potentialities of the simulator and supporting the compatibility with the most recent 5G network technologies. The full *Omnet++* code of the designed model may be requested by sending an email to one of the authors of the present paper.

REFERENCES

Björnson, E., Larsson, E. G., and Debbah, M. (2016). Massive mimo for maximal spectral efficiency: How many users and pilots should be allocated? *IEEE Transactions on Wireless Communications*, 15(2):1293–1308.

Björnson, E., Sanguinetti, L., Hoydis, J., and Debbah, M. (2015). Optimal design of energy-efficient multi-user mimo systems: Is massive mimo the answer? *IEEE Transactions on Wireless Communications*, 14(6):3059–3075.

Carneiro, G. (2010). Ns-3: Network simulator 3. In *UTM Lab Meeting April*, volume 20.

Chunjian, L. (2003). Efficient antenna patterns for three-sector wcdma systems. *Master of Science Thesis, Chalmers University of Technology, Göteborg, Sweden*.

De Rango, F., Gerla, M., and Marano, S. (2006). A scalable routing scheme with group motion support in large and dense wireless ad hoc networks. *Computers & Electrical Engineering*, 32(1-3):224–240.

De Rango, F., Lonetti, P., and Marano, S. (2008). Mea-dsr: a multipath energy-aware routing protocol for wireless

ad hoc networks. In *Advances in Ad Hoc Networking*, pages 215–225. Springer.

El Ayach, O., Rajagopal, S., Abu-Surra, S., Pi, Z., and Heath, R. W. (2014). Spatially sparse precoding in millimeter wave mimo systems. *IEEE transactions on wireless communications*, 13(3):1499–1513.

Fazio, P., De Rango, F., and Sottile, C. (2011). A new interference aware on demand routing protocol for vehicular networks. In *Performance Evaluation of Computer & Telecommunication Systems (SPECTS), 2011 International Symposium on*, pages 98–103. IEEE.

Fazio, P., De Rango, F., and Sottile, C. (2012). An on demand interference aware routing protocol for vanets. *JNW*, 7(11):1728–1738.

Gao, X., Edfors, O., Rusek, F., and Tufvesson, F. (2015). Massive mimo performance evaluation based on measured propagation data. *IEEE Transactions on Wireless Communications*, 14(7):3899–3911.

Inzillo, V., De Rango, F., and Quintana, A. A. (2017a). A new variable error metric adaptive beamforming algorithm for smart antenna systems. In *Wireless Communications and Mobile Computing Conference (IWCMC), 2017 13th International*, pages 1195–1200. IEEE.

Inzillo, V., De Rango, F., Santamaria, A. F., and Quintana, A. A. (2017b). A new switched beam smart antenna model for supporting asymmetrical communications extending inet omnet++ framework. In *Performance Evaluation of Computer and Telecommunication Systems (SPECTS), 2017 International Symposium on*, pages 1–7. IEEE.

Jain, M. and Agarwal, R. (2016). Capacity & coverage enhancement of wireless communication using smart antenna system. In *Advances in Electrical, Electronics, Information, Communication and Bio-Informatics (AEEICB), 2016 2nd International Conference on*, pages 310–313. IEEE.

Janota, A., Šimák, V., Nemec, D., and Hrbček, J. (2015). Improving the precision and speed of euler angles computation from low-cost rotation sensor data. *Sensors*, 15(3):7016–7039.

Jungnickel, V., Manolakis, K., Zirwas, W., Panzner, B., Braun, V., Lossow, M., Sternad, M., Apelfrojd, R., and Svensson, T. (2014). The role of small cells, coordinated multipoint, and massive mimo in 5g. *IEEE Communications Magazine*, 52(5):44–51.

Kumar, N. A., Rao, S. R., and Rao, V. S. (2014). Analysis of performance improvement in adaptive beam forming using rlms algorithm in smart antenna systems (sas). *International Journal of Research in Science and Technology*, 1(9).

Larsson, E. G., Edfors, O., Tufvesson, F., and Marzetta, T. L. (2014). Massive mimo for next generation wireless systems. *IEEE communications magazine*, 52(2):186–195.

Lu, L., Li, G. Y., Swindlehurst, A. L., Ashikhmin, A., and Zhang, R. (2014). An overview of massive mimo: Benefits and challenges. *IEEE journal of selected topics in signal processing*, 8(5):742–758.

Mezzavilla, M., Dutta, S., Zhang, M., Akdeniz, M. R., and Rangan, S. (2015). 5g mmwave module for the ns-3 network simulator. In *Proceedings of the 18th ACM International Conference on Modeling, Analysis and Simulation of Wireless and Mobile Systems*, pages 283–290. ACM.

Molisch, A. F., Ratnam, V. V., Han, S., Li, Z., Nguyen, S. L. H., Li, L., and Haneda, K. (2017). Hybrid beamforming for massive mimo: A survey. *IEEE Communications Magazine*, 55(9):134–141.

Nguyen, H.-S., Do, D.-T., and Voznak, M. (2016a). Two-way relaying networks in green communications for 5g: Optimal throughput and tradeoff between relay distance on power splitting-based and time switching-based relaying swipt. *AEU-International Journal of Electronics and Communications*, 70(12):1637–1644.

Nguyen, T. N., Duy, T. T., Tran, P. T., and Voznak, M. (2016b). Performance evaluation of user selection protocols in random networks with energy harvesting and hardware impairments. *Advances in Electrical and Electronic Engineering*, 14(4):372–377.

Ohta, K. and Ishida, H. (1988). Comparison among several numerical integration methods for kramers-kronig transformation. *Applied Spectroscopy*, 42(6):952–957.

Omnet++ (2018). 5.3 release.

Pei, G. and Henderson, T. R. (2010). Validation of ofdm error rate model in ns-3. *Boeing Research Technology*, pages 1–15.

Senapati, A., Ghatak, K., and Roy, J. S. (2015). A comparative study of adaptive beamforming techniques in smart antenna using lms algorithm and its variants. In *Computational Intelligence and Networks (CINE), 2015 International Conference on*, pages 58–62. IEEE.

Tan, W., Assimonis, S. D., Matthaiou, M., Han, Y., Li, X., and Jin, S. (2017). Analysis of different planar antenna arrays for mmwave massive mimo systems.

Yan, H. and Cabric, D. (2017). Digital predistortion for hybrid precoding architecture in millimeter-wave massive mimo systems. In *Acoustics, Speech and Signal Processing (ICASSP), 2017 IEEE International Conference on*, pages 3479–3483. IEEE.

Yang, G., Ho, C. K., Zhang, R., and Guan, Y. L. (2015). Throughput optimization for massive mimo systems powered by wireless energy transfer. *IEEE Journal on Selected Areas in Communications*, 33(8):1640–1650.

Zhang, H., Liu, N., Chu, X., Long, K., Aghvami, A.-H., and Leung, V. C. (2017). Network slicing based 5g and future mobile networks: mobility, resource management, and challenges. *IEEE Communications Magazine*, 55(8):138–145.

Zhang, J. A., Huang, X., Dyadyuk, V., and Guo, Y. J. (2015). Massive hybrid antenna array for millimeter-wave cellular communications. *IEEE Wireless Communications*, 22(1):79–87.

Zhou, B., Lee, Y.-Z., Gerla, M., and De Rango, F. (2006). Geo-lanmar: a scalable routing protocol for ad hoc networks with group motion. *Wireless Communications and Mobile Computing*, 6(7):989–1002.